Evaluation of Treatment Response of Chemoembolization in Hepatocellular Carcinoma with Diffusion-Weighted Imaging on 3.0-T MR Imaging

Hilal Sahin, MD, Mustafa Harman, MD, Celal Cinar, MD, Halil Bozkaya, MD, Mustafa Parildar, MD, and Nevra Elmas, MD

ABSTRACT

Purpose: To assess the treatment response of hepatocellular carcinoma (HCC) after transarterial chemoembolization with diffusion-weighted imaging and dynamic contrast-enhanced magnetic resonance (MR) imaging with a 3-T system.

Materials and Methods: Between February 2010 and November 2010, 74 patients were treated with chemoembolization in our interventional radiology unit. Twenty-two patients (29%) who had liver MR imaging including diffusion and dynamic contrast-enhanced MR imaging on a 3-T system before and after transarterial chemoembolization were evaluated retrospectively. Tumor size, arterial enhancement, venous washout, and apparent diffusion coefficient (ADC) values of lesions, peritumoral parenchyma, normal liver parenchyma, and spleen were recorded before and after treatment. The significance of differences between ADC values of responding and nonresponding lesions was calculated.

Results: The study included 77 HCC lesions (mean diameter, 31.4 mm) in 20 patients. There was no significant reduction in mean tumor diameter after treatment. Reduction in tumor enhancement in the arterial phase was statistically significant ($P = .01$). Tumor ADC value increased from 1.10×10^{-3} mm^2/s to 1.27×10^{-3} mm^2/s after treatment ($P < .01$), whereas the ADC values for liver and spleen remained unchanged. ADC values from cellular parts of the tumor and necrotic areas also increased after treatment. However, pretreatment ADC values were not reliable to identify responding lesions according to the results of receiver operating characteristic analysis.

Conclusions: After transarterial chemoembolization, responding HCC lesions exhibited decreases in arterial enhancement and increases in ADC values in cellular and necrotic areas. Pretreatment ADC values were not predictive of response to chemoembolization.

ABBREVIATIONS

ADC = apparent diffusion coefficient, AFP = α-fetoprotein, DWI = diffusion-weighted imaging, HCC = hepatocellular carcinoma, PD = progressive disease, PR = partial response, RECIST = Response Evaluation Criteria In Solid Tumors, ROC = receiver operating characteristic, ROI = region of interest, TE = echo time, TR = repetition time

Tumor response after image-guided transcatheter therapy in hepatocellular carcinoma (HCC) is monitored by tumor markers, radiologic imaging, or histologic analysis. Doppler ultrasonography, computed tomography (CT), and magnetic resonance (MR) imaging have been used to evaluate treatment response radiologically (1). In oncology, Response Evaluation Criteria In Solid Tumors (RECIST) have been used to measure therapeutic response; these criteria rely on changes in the size of lesions. However, new locoregional therapies in HCC aim to achieve tumor necrosis rather than tumor disappearance (2). With the realization that anatomy may not change after locoregional therapies, new evaluation methods based on cellular or molecular changes have been devised. These methods, such as perfusion MR imaging, diffusion-weighted imaging (DWI), and MR spectroscopy, focus on assessment of tumor vascular

From the Department of Radiology, Ege University Faculty of Medicine, 35100 Bornova, Izmir, Turkey. Received May 26, 2011; final revision received August 24, 2011; accepted August 25, 2011. Address correspondence to H.S.; E-mail: hilalcimen@gmail.com

None of the authors have identified a conflict of interest.

J Vasc Interv Radiol 2012; 23:241–247

DOI: 10.1016/j.jvir.2011.08.030

and cellular integrity, motion of water molecules, and biochemical concentrations (1).

In daily practice, CT and MR imaging are valuable in the evaluation of tumor response after locoregional therapies in HCC. New updated guidelines of the American Association for the Study of Liver Disease recommend contrast-enhanced CT or MR imaging to monitor treatment response (3). However, it is sometimes difficult to determine enhancing residual tumor tissue because of hyperattenuating iodized oil on CT studies. Areas of enhanced contrast in the arterial phase indicate viable tumor tissue, but differentiation of granulation tissue from viable tumor tissue is not always easy on MR imaging studies (1).

DWI is a recently studied technique in tumor response evaluation that determines motion of water molecules in tissue. In the past, it was used only in cranial examinations, but with investigation of ultrafast single-shot echoplanar imaging, it has been widely used in abdominal studies (1). In addition to many studies about the role of DWI in differential diagnosis of liver lesions, this technique has also recently become popular in tumor response evaluation. Geschwind et al (4) studied diffusion MR imaging in rabbit tumor models after chemoembolization in 2000. They demonstrated that areas with high signal intensity on DWI and low apparent diffusion coefficient (ADC) values corresponded to residual viable tumor tissue. Later studies in humans demonstrated that ADC values before and after transcatheter therapy can distinguish necrotic tissue from viable tumor (5,6). There have been few studies of ADC increases after transarterial chemoembolization procedure on high-field MR imaging (4,7,8). Chen et al (7) suggested that hepatic choline levels and ADC may allow monitoring of responses of large HCC to transarterial chemoembolization in the early period (2–3 d) after chemoembolization. Lu et al (8) studied intraobserver and interobserver variability in treated malignant lesions on a 3.0-T MR system. The present study was performed to assess the treatment response of HCC 1 month after image-guided transcatheter therapy with DWI and dynamic contrast-enhanced MR imaging on a 3.0-T system in a relatively large group of HCCs and to compare the two imaging techniques.

MATERIALS AND METHODS

Patient Selection

Patients who underwent a transarterial chemoembolization procedure between February 2010 and October 2010 in a single interventional radiology department were retrospectively evaluated. Institutional review board approval was obtained. Inclusion required (i) a diagnosis of HCC and (ii) contrast-enhanced dynamic MR imaging and DWI studies within 10 days before chemoembolization and 21–50 days afterward on a 3.0-T MR imaging unit.

In a period of 8 months, image-guided transcatheter tumor therapy was administered to 74 patients. Among 74 patients, only 22 had MR studies in the 3.0-T unit before and after treatment. The other 52 patients were excluded because they had CT studies or MR imaging studies in a 1.5-T system before or after treatment. After excluding one patient with diagnosis of liver hemangioma and one patient with colon cancer liver metastasis, 20 patients (12 men, eight women; age range, 41–75 y; mean age, 61 y) were included in the study. Barcelona Clinic Liver Cancer guidelines were used for diagnosis of HCC (9). Patients had dynamic abdominal CT during the 3 months before chemoembolization, and diagnosis was confirmed by CT and pretreatment MR imaging. Biopsy was not performed if the enhancement pattern was typical for HCC on both imaging modalities and there was an elevated α-fetoprotein (AFP) level. In two atypical lesions, diagnosis was proven by biopsy. To differentiate HCC from dysplastic or regenerative nodules, MR signals and typical arterial enhancement on previous CT or MR images were analyzed. When differentiation was difficult in small lesions, hepatocellular contrast agent (gadolinium ethoxybenzyl diethylenetriaminepentaacetic acid) was used for the diagnosis of HCC. In all patients, response to one image-guided transcatheter therapy procedure was evaluated (first procedure in eight patients; second, third, and fourth in three each; fifth in two; and sixth in one). Medical data including liver function test results (aspartate and alanine aminotransferases, alkaline phosphatase γ-glutamyltranspeptidase, albumin, and total and direct bilirubin) and AFP levels before and after treatment were also recorded.

Liver MR Imaging Technique

All patients included in the study had dynamic liver MR imaging and DWI in a high-gradient (maximum gradient, 40 mT/m; maximum slew rate, 200 mT/m/s) 3.0-T unit (Verio; Siemens, Erlangen, Germany). An eight-channel phased-array coil was used anteriorly and two groups of four-channel fixed spine coils were used posteriorly. By the use of total imaging matrix technology, studies was performed by using 12 or 16 channels (according to the length of examination area) in total.

MR imaging protocol included a coronal half-Fourier acquisition single-shot turbo spin-echo sequence for planning, spin-echo T2-weighted BLADE sequence (BLADE is the Siemens Medical Solutions implementation of periodically rotated overlapping parallel lines with enhenced reconstruction sequence) (repetition time [TR]/echo time [TE], 2,500 ms/89 ms; flip angle, 140°; matrix, 256 × 320; slice thickness, 6 mm; slice gap, 0 mm; one excitation; field of view, 35–40 cm), and dynamic three-dimensional gradient-echo volumetric interpolated breath-hold examination sequence (TR/TE, 3.92 ms/1.39 ms; flip angle, 9°; matrix, 224 × 320; slice thickness, 3 mm; slice gap, 0 mm; one excitation; 64 slices) with parallel imaging algorithm (generalized autocalibrating partially parallel acquisitions factor of 2) and an 18-second breath-hold period in early, late arterial, and portal phases.

DWI was applied before dynamic study with single-shot echoplanar imaging and respiratory triggering tech-

nique in axial plane. b-Values were 50, 400, and 800 s/mm^2. Other parameters were as follows: TR/TE, 6,200 ms/72 ms; matrix, 102 × 128; slice thickness, 6 mm; slice gap, 0 mm; six excitations; field of view, 38 cm; and slice number, 90 (30 slices for each b-value; bandwidth, 2,442 kHz). Spectral fat-saturation technique (ie, spectral attenuated inversion recovery) and a parallel imaging algorithm (generalized autocalibrating partially parallel acquisitions factor of 2) were used. A mean ADC map was constituted with isotropic images automatically.

Chemoembolization Technique

Fluoroscopy-guided transcatheter tumor therapy was performed by three interventional radiologists with 3, 5, and 10 years of clinical experience in chemoembolization. An emulsion of doxorubicin (1 mg/kg; Teva, Irvine, California) was dissolved in 5 mL of nonionic contrast material (Omnipaque 350/100; Amersham, Piscataway, New Jersey) and 10 mL of iodized oil (Lipiodol Ultra Fluid; Laboratoire Andre Guerbet, Aulnay-sous-Bois, France), which was administered slowly under fluoroscopic guidance to avoid reflux.

In two patients, drug-eluting beads (DC Bead; Biocompatibles, Farnham, United Kingdom) were used for chemoembolization. In one patient, 150–250-μm polyvinyl alcohol particle infusion was applied before and after chemoembolization as a result of the presence of an arterioportal fistula.

Image Analysis

MR studies of 77 HCC lesions larger than 1 cm in 20 patients were evaluated retrospectively from an electronic archive system. Dimension, internal structure (ie, homogenous or heterogenous appearance, presence of hemorrhage, fatty metamorphosis, fibrosis), T1 and T2 signal intensity, enhancement in the arterial phase, and washout of each lesion were evaluated before and after chemoembolization. Tumor response was evaluated by two radiologists (H.S. and M.H.) with consensus based on initial contrast-enhanced MR imaging (1 mo after chemoembolization), and results was confirmed by subsequent follow-up MR images, which were repeated every 2–3 months. Response was defined according to modified RECIST and classified into four grades as follows: complete response indicated disappearance of any intratumoral enhancement in all target lesions; partial response (PR) indicated a decrease of at least 30% in the sum of greatest dimension of viable (ie, enhancing) target lesions; progressive disease (PD) indicated an increase of at least 20% in the sum of the greatest dimension of viable (ie, enhancing) target lesions, and stable disease indicated tumor response between PR and PD (10). Then, lesions were grouped as "responding," including complete response and PR, or "nonresponding," including PD and stable disease.

Diffusion-weighted MR images were reviewed on a postprocessing workstation (Leonardo; Siemens), and a region of interest (ROI) was placed over the entire area of the treated mass as seen on an axial image with maximum size. In heterogenous lesions, a standard ROI with minimum size (0.44 cm^2) was also placed on mostly diffusion-restricted areas with low signal (corresponding to cellular areas) and increased-diffusion areas with high signal (corresponding to necrotic areas) in the ADC map. Mean ADC values were calculated after three measurements for each area. In addition, ADC measurements from three different places around each tumoral lesion were established. For the evaluation of normal-appearing liver parenchyma and spleen, standard ROIs were randomly drawn from five different slices. Mean ADCs of normal liver and spleen before and after chemoembolization were compared. Artifacts caused by physical limitations related to higher field strength or image protocols were also noted.

Statistical Analysis

Statistical analysis was performed with SPSS software (version 15.0; IBM, Armonk, New York). Pretreatment and posttreatment mean, minimum, and maximum ADC values of the lesions and ADC values around the tumors were evaluated by Wilcoxon signed-rank test. Correlation between treatment response and differences in ADC values was evaluated by Mann–Whitney U test. Receiver operating characteristic (ROC) analysis was performed to determine a threshold ADC to differentiate responding lesions from nonresponding lesions. Mean ADC values of the liver parenchyma and spleen, liver function test results, and AFP levels before and after treatment were also compared by Wilcoxon signed-rank test. Differences were considered significant when P values were less than .05.

RESULTS

Twenty patients who met the inclusion criteria were evaluated retrospectively. Transarterial chemoembolization procedures were selective in 18 patients (16 right hepatic artery segmental/subsegmental branch, one left hepatic artery segmental branch, one left phrenic artery) and nonselective in two patients (from proper hepatic artery) in view of multiplicity of lesions in both lobes and inappropriate vascular access to lesions. The mean duration between pretreatment MR imaging and transcatheter tumor therapy was 1 day (range, 0–9 d), and mean duration between therapy and posttreatment MR imaging was 33 days (range, 24–49 d).

Mean tumor size was 31.4 mm (range, 10–155 mm) before treatment and was 31.5 mm (range, 9–156 mm) after treatment. Differences in mean tumor size were not significant (P = .704). A total of 63 lesions (81.8%) were homogenous in internal structure, and 14 (18.2%) were heterogenous. There was no remarkable hemorrhage, fatty metamorphosis, or fibrosis in any of the lesions. A total of 67 lesions (87%) had contrast enhancement in the arterial phase, and 73 (94.8%) had venous washout (by 60 s after contrast agent administration) before treatment. Arterial

Table. ADC Measurements before and after Chemoembolization

	ADC Value ($\times 10^{-3}$ mm^2/s)			
	Before Chemoembolization		After Chemoembolization	
Parameter	Range	Mean	Range	Mean
Tumor (total)	0.73–1.81	1.10	0.81–1.98	1.27
Viable tumor	0.64–1.04	0.84	0.63–1.19	0.98
Necrosis	1.21–1.93	1.53	1.51–3.20	1.92
Around tumor	0.83–1.59	1.15	0.77–1.92	1.23

Note.—ADC = apparent diffusion coefficient.

enhancement disappeared in nine lesions after treatment, which was statistically significant ($P < .05$), but changes in venous washout were not significant ($P = 1.00$). After evaluation of posttreatment initial contrast-enhanced and follow-up MR imaging studies, 40 lesions (51.9%) were accepted as responding to transcatheter therapy.

Mean tumor total ADC value was 1.10×10^{-3} mm^2/s ± 0.21 on MR imaging before chemoembolization (**Table**). After treatment, this value increased to 1.27×10^{-3} mm^2/s ± 0.25. ADC values increased in 62 lesions, decreased in 13, and stayed stable in two (**Fig 1**). The increase in mean ADC value was calculated as 15.4%. Changes in mean tumor ADC values were significant according to Wilcoxon signed-rank test ($P < .01$), whereas the mean ADC values for liver and spleen remained unchanged (liver, 1.16×10^{-3} mm^2/s ± 0.10 vs 1.13×10^{-3} mm^2/s ± 0.15; spleen, 0.93×10^{-3} mm^2/s ± 0.17 vs 0.94×10^{-3} mm^2/s ± 0.16 before and after treatment, respectively). When AFP and liver function test results before and after image-guided transcatheter tumor therapy were compared, there were no significant differences either.

Mean ADC measurement from lowest signal intensity areas (ie, cellular parts) of 14 heterogenous lesions also increased after treatment (**Table**). In 12 of the 14 lesions (85%), ADC values of the most cellular areas increased after treatment, whereas they decreased in two lesions (15%). Differences of ADC values of cellular parts of the tumor were statistically significant before versus after treatment ($P = .02$). In heterogenous lesions, high signal areas on ADC maps were assessed as necrosis in correlation with T2-weighted images. ADC measurements from those areas also significantly increased according to Wilcoxon signed-rank test ($P < .01$; **Table**). Similarly, the mean ADC value of the peritumoral liver parenchyma increased after treatment according to Wilcoxon signed-rank test, indicating chemoembolization-induced histopathologic changes (eg, inflammation, granulation tissue, congested sinusoids; $P < .01$; **Table**). However, those changes were not proven pathologically, as patients were not candidates for lesion resection or liver transplantation.

There was a strong relation between differences in tumor ADC values and treatment response according to Mann–Whitney U test ($P < .01$). ADC values increased in responding lesions whereas they did not change in nonresponding lesions (**Fig 2**). In addition, results of ROC analysis for nonresponding versus responding lesions and pretreatment ADC values were not significant ($P = .81$; **Fig 3**). The area under the curve was 0.48.

When differences in size and ADC values of the lesions were compared, significant negative correlation was found between them ($P < .01$). There was also a negative correlation between those parameters in the responding lesion group ($P < .01$), but the relation was not significant for the nonresponding lesion group ($P = .18$).

DISCUSSION

Response assessment is crucial in directing cancer therapy, as it is an important factor effecting survival rate. To inform the decision to continue, interrupt, or finish transcatheter tumor therapy, treatment response should be evaluated reliably. In time, it has become evident that RECIST standards are not enough for response evaluation in HCC because they do not take into account changes in tumor viability that may be associated with tumor response (11). However, in HCC, the goal of local treatment is tumor necrosis rather than tumor shrinkage. Tumor size may not parallel the ratio of necrosis even if a large degree of necrosis occurs in the tumor. In the present study, differences in tumor size were not significant, as we expected. In 2000, the European Association for the Study of the Liver (12) proposed that the optimal method to evaluate response to local treatment is to assess the decrease in viable tumor volume, which is seen as a decrease in enhancing areas on contrast-enhanced images. Homogenous, thin rim enhancement around tumor on delayed gadolinium-enhanced images represents chemoembolization-induced vasculitis, inflammation, and granulation tissue after local treatment (13). Contrast enhancement in granulation tissue is believed to be caused by increased capillary permeability and increased distribution of gadolinium (14). On the contrary, the presence of nodular ring enhancement should cast doubt on local progression. In those situations, DWI may have a promising role in the differentiation of necrosis and viable tumor, as ADC values increase in the presence of necrosis (15).

Response assessment is a newly developing scope of DWI that does not require the use of contrast media. The first studies of this issue were done in rabbit VX2 tumor models (4,16). According to those studies, necrotic areas have higher ADC values than viable tumor areas, and ADC of normal liver parenchyma and VX2 tumor are influenced by intracellular edema, tissue cellular death, and microcirculation disturbance after chemoembolization. Kamel et al (5) demonstrated increase in ADC values with increasing tumor necrosis in eight patients with HCC, with pathologic correlation. After 3 years, another study of the same authors (17) demonstrated that mean ADC values of 38 lesions

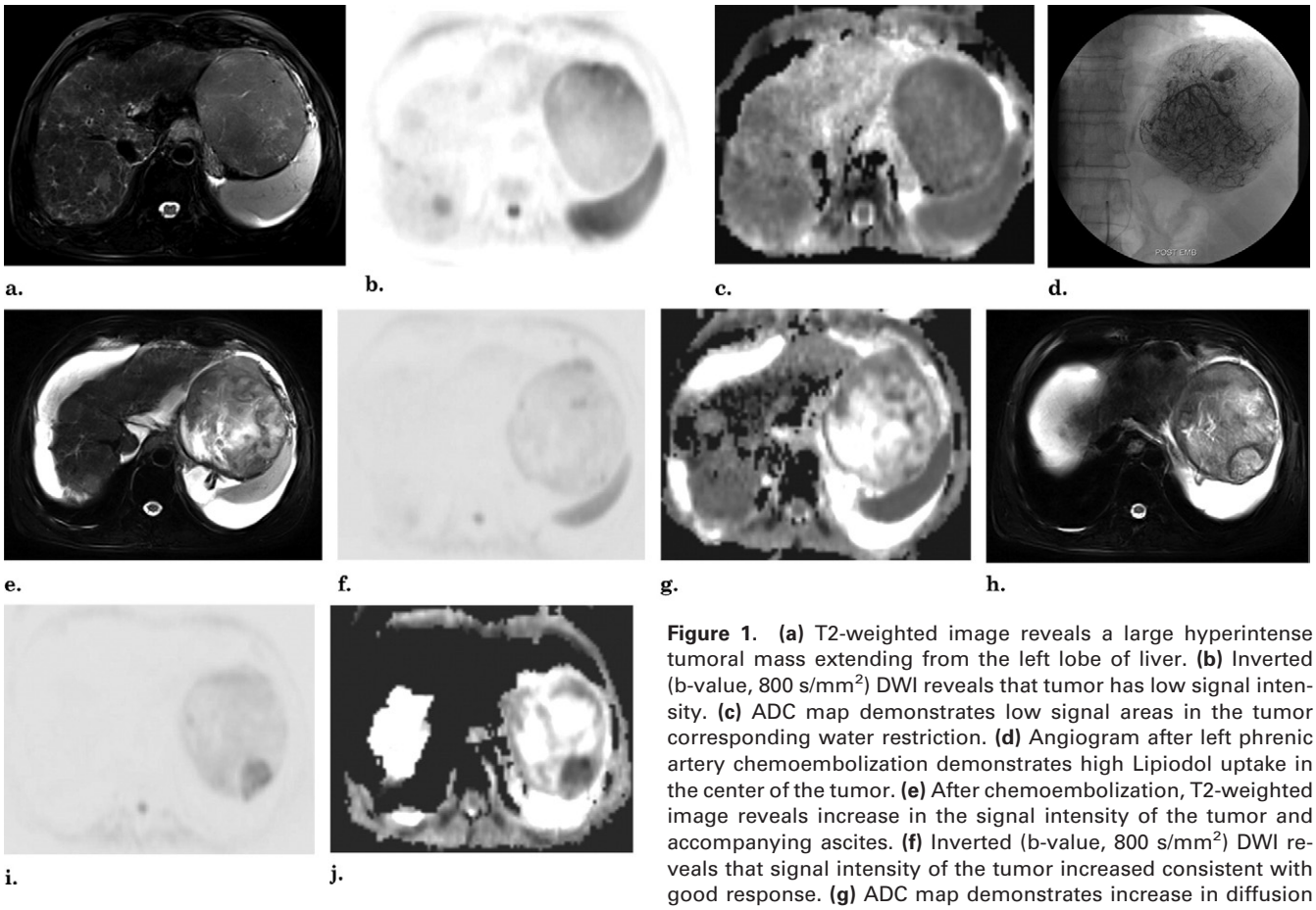

Figure 1. **(a)** T2-weighted image reveals a large hyperintense tumoral mass extending from the left lobe of liver. **(b)** Inverted (b-value, 800 s/mm^2) DWI reveals that tumor has low signal intensity. **(c)** ADC map demonstrates low signal areas in the tumor corresponding water restriction. **(d)** Angiogram after left phrenic artery chemoembolization demonstrates high Lipiodol uptake in the center of the tumor. **(e)** After chemoembolization, T2-weighted image reveals increase in the signal intensity of the tumor and accompanying ascites. **(f)** Inverted (b-value, 800 s/mm^2) DWI reveals that signal intensity of the tumor increased consistent with good response. **(g)** ADC map demonstrates increase in diffusion in the center of the tumor representing necrosis. **(h)** T2-weighted image shows that the tumoral mass has a hyperintense area posteriorly circumscribed with a hypointense rim in the more cranial part. **(i)** Inverted (b-value, 800 s/mm^2) DWI reveals low signal in the area apart from necrosis. **(j)** ADC map demonstrates water restriction at the posterior part of the tumor consistent with viable tumor.

increased from 1.5×10^{-3} mm^2/s to 1.8×10^{-3} mm^2/s even though the change in percentage of tumor size did not fulfill RECIST for complete or partial response. According to the present results, change in tumor size was not a prognostic factor in determining response. In addition, mean tumor ADC value increased from 1.10×10^{-3} mm^2/s to 1.27×10^{-3} mm^2/s in the present study. ADC values obtained were lower than the ADC values of the lesions in the studies of Kamel et al (5,17), and this may be a consequence of differences in parameters of DWI and magnetic strength in our opinion. Also of note is the difference in percentage of ADC increase. In their study (17), increase in ADC was 20%, whereas, in the present study, it was 15.4%. We conclude that this difference occurred because most lesions in the present study were treated with one or more image-guided transcatheter tumor therapy procedures previously and already had necrotic areas.

Yuan et al (14) proposed that high pretreatment mean ADC values of HCC were predictive of poor response to chemoembolization. In their study of 25 responding and nine nonresponding lesions, the threshold ADC value of 1.618×10^{-3} mm^2/s had 96.0% sensitivity and 77.8% specificity for identification of nonresponding lesions according to ROC analysis. Conversely, this analysis to find a threshold ADC value was not significant in the present study ($P = .81$). This may be a result of multiple previous sessions of image-guided transcatheter tumor therapy in 65% of lesions, which caused relatively higher ADC values. Nonetheless, there were more lesions treated in the present study, and the numbers of lesions in the two groups were similar (40 responding lesions and 37 nonresponding lesions). Therefore, our results, based on which we propose that pretreatment ADC values cannot predict response to chemoembolization, may be more meaningful. However, further studies on this issue with larger numbers of patients are needed to reach a firmer conclusion.

There have been few studies of increases in ADC values after transarterial chemoembolization on 3.0-T MR imaging (4,7,8). However, each of these studies had a relatively small sample size, and they used somewhat divergent imaging protocols (eg, different sequences, b-values, and tumor cell lines). In 2000, Geschwind et al (4) assessed the efficacy of image-guided transcatheter tumor therapy in rabbits with VX2 liver tumors and in untreated control rabbits at a high magnetic field. They demonstrated higher ADCs in areas of necrosis than in viable tumor, with

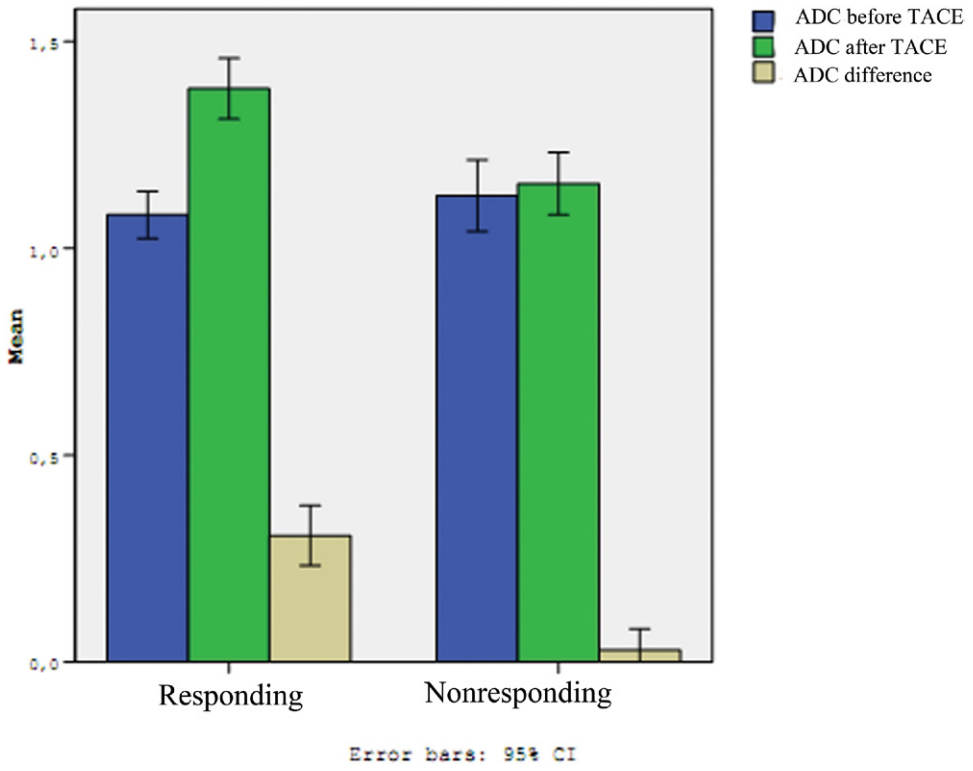

Figure 2. Bar chart demonstrates mean ADC values of the responding and nonresponding lesions before and after treatment. (Available in color online at *www.jvir.org*.)

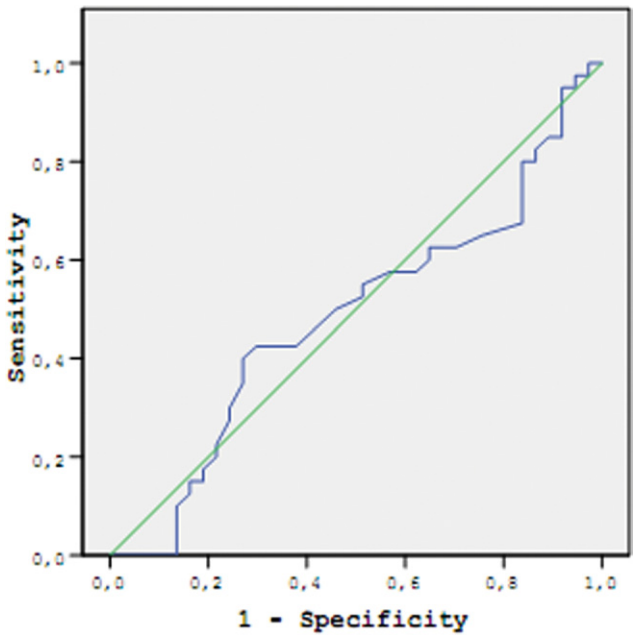

Figure 3. ROC analysis for differentiation of responding and nonresponding lesions with pretreatment ADC values shows no significant difference between groups. (Available in color online at *www.jvir.org*.)

histopathologic conformation on images acquired shortly after the animals' death. However, they were not able to differentiate necrotic and viable tissue clearly with the use of conventional sequences. Although histopathologic correlation was not performed in the present study, necrosis and enhancing viable tumor could be clearly distinguished. This may be the result of improvement in sequence techniques and optimization of protocols in the 10 years since the study of Geschwind et al (4). Chen et al (7) further demonstrated an increase in ADC values (from 1.56 × 10^{-3} mm^2/s to 2.09 × 10^{-3} mm^2/s) as early as 2–3 days after therapy in 20 patients. However, those ADC values, even before treatment, were higher than the mean tumor ADC values in the present study, even though the magnetic fields were similar. We think this difference may be the result of differences in b-values, which were 0 and 500 in the study of Chen et al (7) and 50, 400, and 800 in the present study. Choice of b-values may have influence on calculated ADC value, which is affected by tissue perfusion at low b-values. This may confound measurement of tissue diffusivity and cause higher ADCs by using lower b-values (18). A recent study by Lu et al (8) compared interobserver and intraobserver variability of ADC in treated malignant hepatic lesions on 3.0-T imaging. Although they did not evaluate response, they made ADC measurements from the whole lesions and from the most restricted diffusion area on post-treatment DWI studies and found that a limited variability in ADC measurements does exist. In the present study, ADC measurements were performed by two radiologists in consensus to eliminate interobserver variability–associated bias.

We did not make a comparative study between 1.5-T and 3.0-T imaging, but we noticed that the high resolution

that results from high magnetic strength and dedicated receiver coils was achieved in dynamic MR imaging and DWI, as reported in the literature (19–21). This enabled us to evaluate small lesions located even in the dome. Also with increased signal-to-noise ratio at 3.0 T, sensitivity to areas of restricted diffusion was improved and resolution problems were not remarkable at high b-values. Image distortion from increased magnetic susceptibility often contributes to a loss of image quality at 3.0 T (22–24). Chen et al (7) determined that image distortions were markedly diminished and that "ghost" or aliasing artifacts were not discernible with the use of sensitivity-encoding technique with echoplanar imaging. However, chemical-shift artifacts and eddy current–induced image warping were still present as a limitation in their study (7). In the present study, geometric distortions related to B0 inhomogeneity were not marked, and differentiation between necrotic and viable areas was not difficult in most lesions. However, in two patients with ascites, partial loss in spatial resolution caused by dielectric effects limited evaluation. Another limitation was that, although respiratory triggering technique increased signal-to-noise ratio on DWI, it caused image distortions and increased examination time in six patients with irregular breathing problems.

Besides the technical limitations, the present study itself has several limitations. The most important one is that we could not perform pathologic correlation because patients were not suitable for lesion resection or liver transplantation. In addition, most patients had image-guided transcatheter tumor therapy sessions before the study, and some lesions had preexisting necrosis, which increased ADC values. Therefore, a specific interpretation of DWI is still not easy. In the present study, although we placed the smallest ROI possible in the necrotic and viable parts of the lesions on the ADC map and made three repeated measurements to minimize possible errors, partial volume effects and uncontrollable image noise caused unavoidable errors, especially in small or irregular lesions. Because we had a high number of lesions in the study with a mean diameter greater than 3 cm, we believe this does not severely limit the study findings.

In conclusion, DWI is a promising technique in the response evaluation of HCC after image-guided transcatheter tumor therapy, depending on the capability on microscopic tissue characterization and water restriction. It facilitates distinction between viable and necrotic tumor areas and helps the diagnosis of residual or recurrent tumor. However, pretreatment ADC values could not predict response to therapy according to the present results. Future studies with high magnetic gradient systems with new technical developments are needed to improve the image quality and sensitivity of DWI.

ACKNOWLEDGMENTS

The authors thank Hatice Uluer (Medical Statistics Department, Ege University) for her help in statistical analysis.

REFERENCES

1. Vossen JA, Buijs M, Kamel IR. Assessment of tumor response on MR imaging after locoregional therapy. Tech Vasc Intervent Radiol 2006; 9:125–132.
2. Kamel IR, Bluemke DA. Magnetic resonance imaging of the liver: assessing response to treatment. Top Magn Reson Imaging 2002; 13: 191–200.
3. Bruix J, Sherman M; American Association for the Study of Liver Diseases. Management of hepatocellular carcinoma: an update. Hepatology 2011; 53:1020–1022.
4. Geschwind JF, Artemov D, Abraham S, et al. Chemoembolization of liver tumor in a rabbit model: assessment of tumor cell death with diffusion-weighted MR imaging and histologic analysis. J Vasc Interv Radiol 2000; 11:1245–1255.
5. Kamel IR, Bluemke DA, Ramsey D, et al. Role of diffusion weighted imaging in estimating tumor necrosis after chemoembolization of hepatocellular carcinoma. AJR Am J Roentgenol 2003; 181:708–710.
6. Yu JS, Kim JH, Chung JJ, Kim KW. Added value of diffusion-weighted imaging in the MRI assessment of perilesional tumor recurrence after chemoembolization of hepatocellular carcinomas. J Magn Reson Imaging 2009; 30:153–160.
7. Chen CY, Li CW, Kuo YT, et al. Early response of hepatocellular carcinoma to transcatheter arterial chemoembolization: choline levels and MR diffusion constants—initial experience. Radiology 2006; 239:448–456.
8. Lu TL, Meuli RA, Marques-Vidal PM, Bize P, Denys A, Schmidt S. Interobserver and intraobserver variability of the apparent diffusion coefficient in treated malignant hepatic lesions on a 3.0T machine: measurements in the whole lesion versus in the area with the most restricted diffusion. J Magn Reson Imaging 2010; 32:647–653.
9. Llovet JM, Fuster J, Bruix J. The Barcelona Approach: diagnosis, staging and treatment of hepatocellular carcinoma. Liver Transpl 2004; 10: 115–120.
10. Lencioni R, Llovet JM. Modified RECIST (mRECIST) assessment for hepatocellular carcinoma. Semin Liver Dis 2010; 30:52–60.
11. Forner A, Ayuso C, Varela M, et al. Evaluation of tumor response after locoregional therapies in hepatocellular carcinoma. Cancer 2009; 115: 616–623.
12. Bruix J, Sherman M, Llovet JM, et al. Clinical management of hepatocellular carcinoma. Conclusions of the Barcelona-2000 EASL conference. European Association for the Study of the Liver. J Hepatol 2001; 35:421–430.
13. Semelka RC, Worawattanakul S, Mauro MA, Bernard SA, Cance WG. Malignant hepatic tumors: changes on MRI after hepatic arterial chemoembolization–preliminary findings. J Magn Reson Imaging 1998; 8:48–56.
14. Yuan Z, Ye XD, Dong S, et al. Role of magnetic resonance diffusion-weighted imaging in evaluating response after chemoembolization of hepatocellular carcinoma. Eur J Radiol 2010; 75:e9–e14.
15. Thabet A, Kalva S, Gervais DA. Percutaneous image-guided therapy of intraabdominal malignancy: imaging evaluation of treatment response. Abdom Imaging 2008; 34:593–609.
16. Yuan YH, Xiao EH, Liu JB, et al. Characteristics and pathological mechanism on magnetic resonance diffusion-weighted imaging after chemoembolization in rabbit liver VX-2 tumor model. World J Gastroenterol 2007; 13:5699–5706.
17. Kamel IR, Bluemke DA, Eng J, et al. The role of functional MR imaging in the assessment of tumor response after chemoembolization in patients with hepatocellular carcinoma. J Vasc Interv Radiol 2006; 17:505–512.
18. Taouli B, Koh DM. Diffusion-weighted MR imaging of the liver. Radiology 2010; 254:47–66.
19. Choi JY, Kim MJ, Chung YE, et al. Abdominal applications of 3.0-T MR imaging: comparative review versus a 1.5-T system. Radiographics 2008; 28:e30.
20. Erturk SM, Alberich-Bayarri A, Herrman KA, Marti-Bonmati L, Ros PR. Use of 3.0-T MR imaging for evaluation of the abdomen. Radiographics 2009; 29:1547–1563.
21. Schindera ST, Merkle EM, Dale BM, Delong DM, Nelson RC. Abdominal magnetic resonance imaging at 3.0 T what is the ultimate gain in signal-to-noise ratio? Acad Radiol 2006; 13:1236–1243.
22. Chang KJ, Kamel IR, Macura KJ, Bluemke DA. 3.0-T MR imaging of the abdomen: comparison with 1.5 T. Radiographics 2008; 28:1983–1998.
23. Dietrich O, Reiser MF, Schoenberg SO. Artifacts in 3-T MRI: physical background and reduction strategies. Eur J Radiol 2008; 65:29–35.
24. Barth MM, Smith MP, Pedrosa I, Lenkinski RE, Rofsky NM. Body MR imaging at 3.0 T: understanding the opportunities and challenges. Radiographics 2007; 27:1445–1464.